Supporting Information

Akgun and Khademi 10.1073/pnas.1007240108

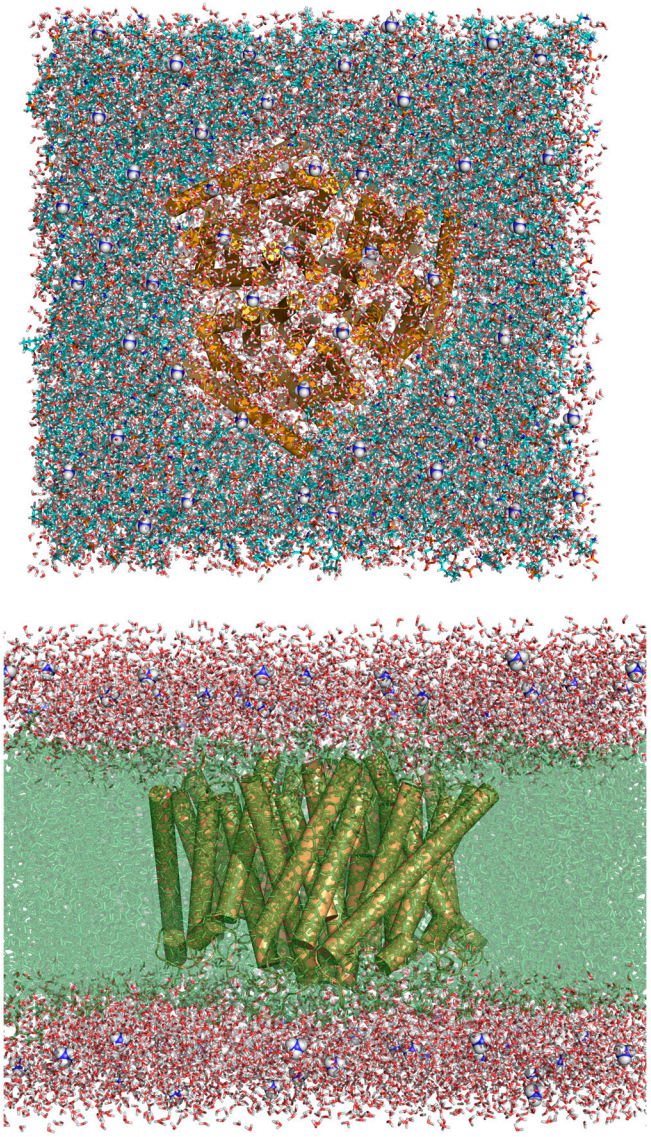

Fig. S1. Top (*Top*) and side (*Bottom*) views of the model used in molecular dynamics (MD) simulations. Trimeric AmtB is shown in gold. phosphatidylethanolamine (POPE) lipid molecules are in transparent green; the NH_4^+ ions and water molecules are shown in van der Waals and stick representations, respectively.

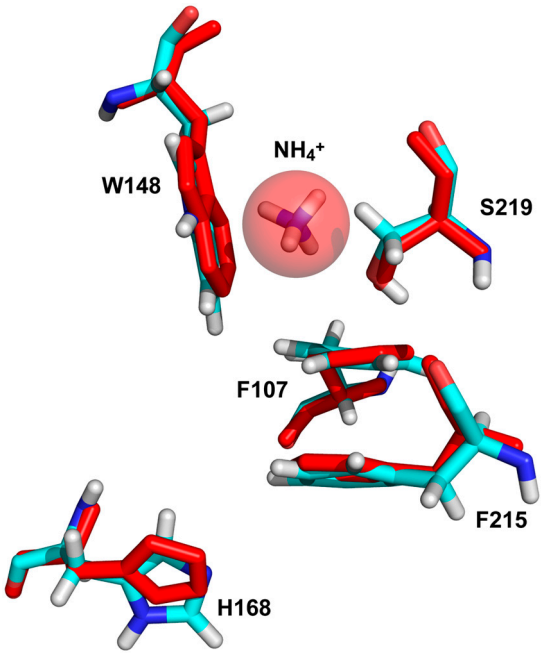

Fig. S2. The Am1 site residues in the crystal structure (Protein Data Bank ID code 1U7G) (red) are superimposed on a snapshot from the MD simulations when NH_4^+ is in the aromatic cage at the bottom of the periplasmic vestibule.

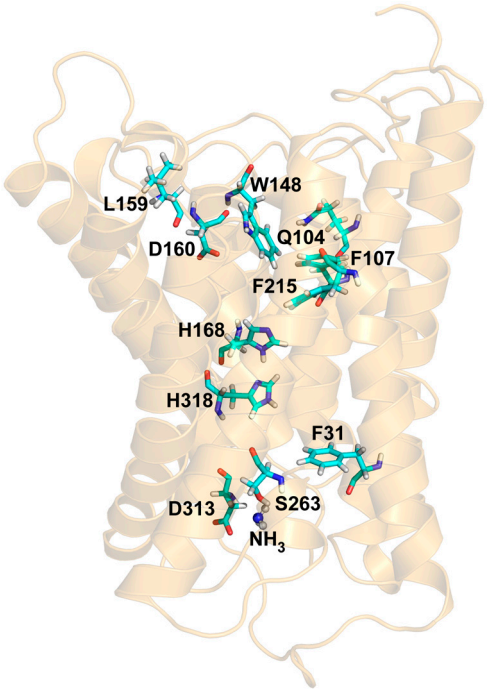

Fig. S3. At the cytoplasmic vestibule, the NH_3 molecule (ball and stick representation) is stabilized by D313 and S263. Some important residues of the periplasmic vestibule are also shown.

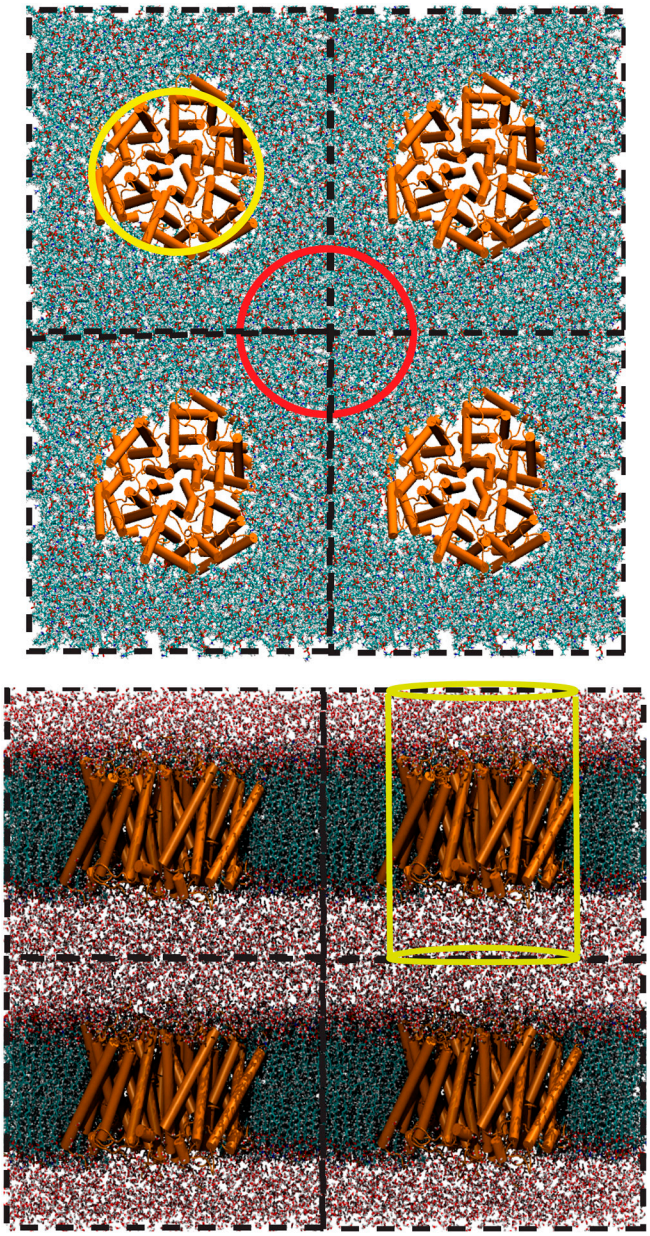

Fig. S4. The top (*Top*) and side (*Bottom*) views of the model show how the hypothetical cylindrical volumes include the trimeric protein (yellow) or membrane regions (red). Dashed lines show the periodic boundaries. The cylindrical volume covering membrane regions occupies four corners of neighboring periodic boundary boxes.

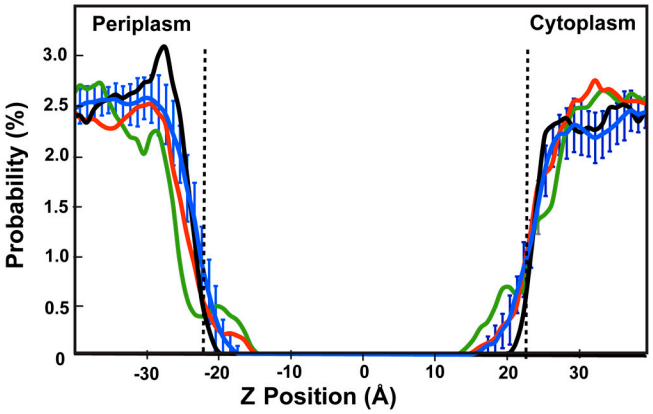

Fig. S5. The solute probability distributions calculated in the cylindrical volume that covers the POPE lipid bilayer. The curves in black, red, blue, and green correspond to NH_4^+, NH_3, H_2O, and CO_2 distributions, respectively. Each point on the water distribution curve is the results of averaging over 10 sets of 100 water molecules. The blue error bars show the standard deviations at each point. The dashed lines indicate the Z coordinate of the phosphate groups of POPE.

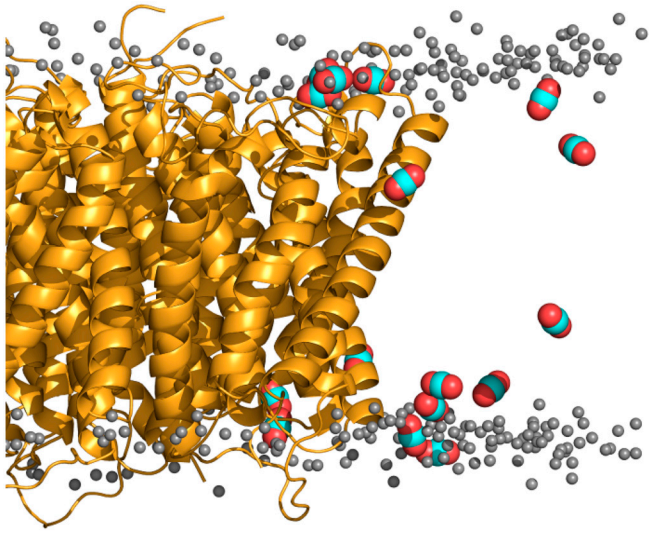

Fig. S6. The CO_2 molecules are penetrating into the POPE lipid bilayer. The phosphates of the lipid head groups are shown with gray spheres. The trimeric AmtB is in orange. The POPE aliphatic tails are not shown.

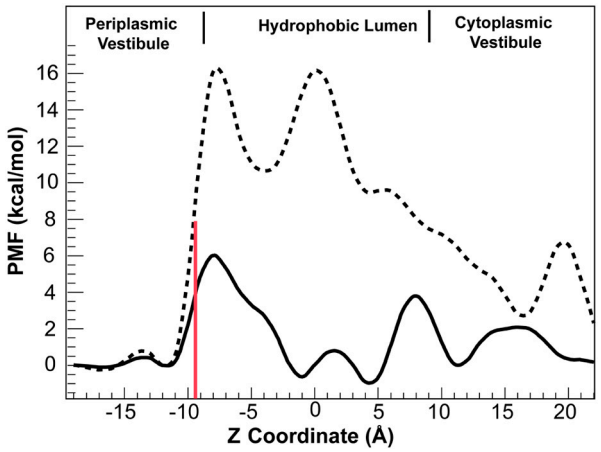

Fig. S7. The energy profile for the conduction of NH_4^+ (dashed line) and NH_3 (solid line) through AmtB channel calculated using steered molecular dynamics simulations. The red line marks where in the pathway the difference between two energy profiles becomes more then 3.75 kcal/mol (the energy needed to lower the ammonia pK_a from 9.25 to 6.5). The difference between two energy profiles ($\Delta\Delta G$) is shown in the Fig. 1C.

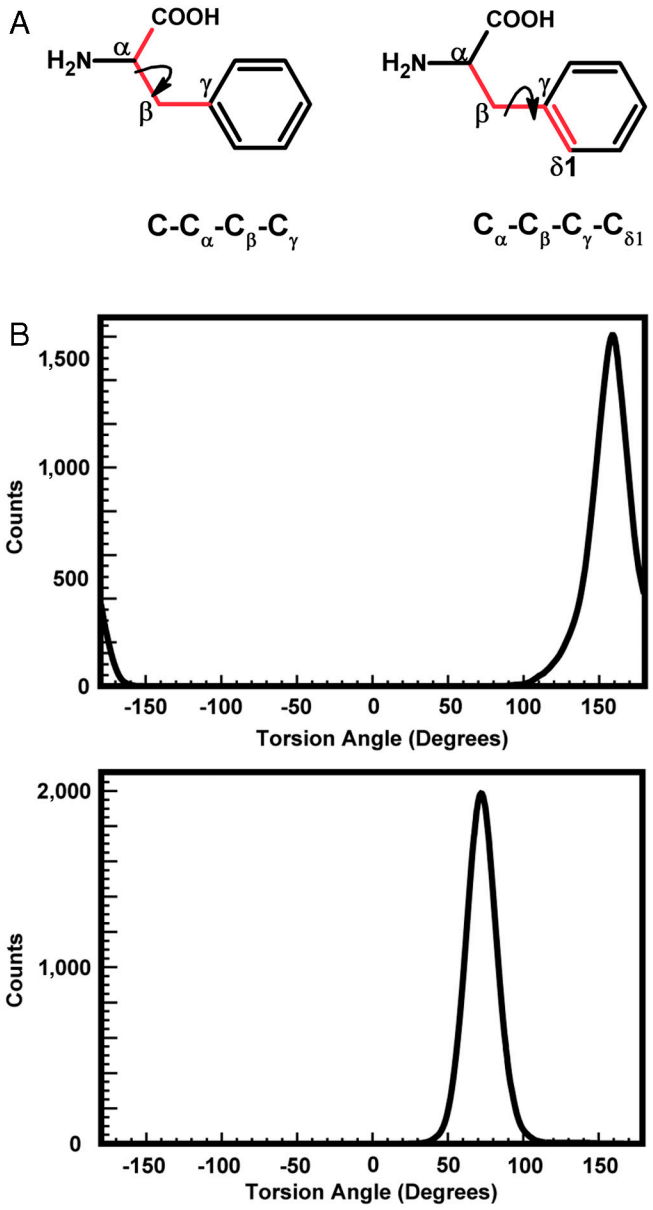

Fig. S8. (*A*) The torsion angles used for the analysis of F107/F215 gating. The red bonds identify the torsion angles of $C\text{-}C_\alpha\text{-}C_\beta\text{-}C_\gamma$ (*Left*) and $C_\alpha\text{-}C_\beta\text{-}C_\gamma\text{-}C_{\delta 1}$ (*Right*). The arrows show the rotating bond for each torsion angle. (*B*) The distributions of the torsion angle $C\text{-}C_\alpha\text{-}C_\beta\text{-}C_\gamma$ for F107 (*Top*) and F215 (*Bottom*).

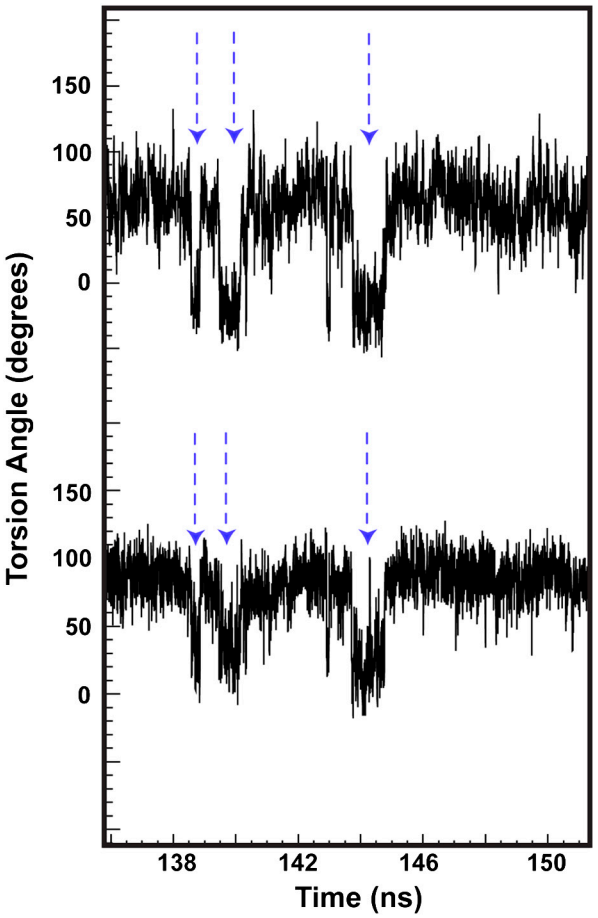

Fig. S9. A sample plot of C_{α}-C_{β}-C_{γ}-$C_{\delta 1}$ torsion angle vs. time demonstrates the synchronized flipping of the phenyl rings of F107 (*Top*) and F215 (*Bottom*). The open states for each phenyl ring are shown with arrows.